POLISH MARITIME RESEARCH 1 (105) 2020 Vol. 27; pp. 107-115
10.2478/pomr-2020-0011

CALCULATION OF THE DYNAMIC CHARACTERISTICS OF SHIP'S AFT STERN TUBE BEARING CONSIDERING JOURNAL DEFLECTION

Hongjun Yang
Shanghai Merchant Ship Design & Research Institute, China
Jun Li
Shanghai Merchant Ship Design & Research Institute, China
Xiaolong Li
Nantong COSCO KHI Ship Engineering Co.,Ltd., China

ABSTRACT

Dynamic properties are vital for the working reliability of aft stern tube bearings. However, the determination of such properties currently involves several simplifications and assumptions. To obtain its dynamic characteristics accurately, the aft stern tube bearing was divided into several bearing segments. The oil film reaction force was considered in the calculation of shaft alignment, and the journal deflection and actual oil film thickness were obtained accordingly. Subsequently, the perturbed Reynolds equation was solved using the finite difference method when the dynamic characteristics of journal bearings with finite width were evaluated. Then, a calculation program was developed and verified by comparing with the results of other studies. Finally, the dynamic characteristics were calculated under different revolutions. The results showed that the stiffness at the vertical direction of the aft stern tube bearing was several times that of the horizontal direction and varied with the revolutions of the shafting system. These findings can provide the foundation for the precise calculation of the journal trajectory under dynamic conditions, as well as for the evaluation of the oil film thickness. Moreover, the results led to favorable conditions for the accurate calculation of the shafting whirling vibration.

Keywords: journal deflection, aft stern tube bearing, dynamic characteristic.

INTRODUCTION

Large merchant ships often adopt low-speed two-stroke diesel engines to directly drive single propellers. The aft stern tube bearings play an important role in the propulsion shafting of ships. In recent years, with the trend towards large-scale ships, as well as the pursuit of navigation economy, the power of the main propulsion has increased with the use of low-speed and large-diameter propellers in propulsion systems. The propeller weight and unbalanced force caused by the uneven wake at the stern of the ship are increasing, thereby highlighting the effect of edge load on the aft stern tube bearing, which increases the risk of failure.

Under extreme working conditions, such as the partial immersion of propellers and the turning test of ships, a high temperature might occur in the aft stern tube bearing. Since 2014, when environmentally acceptable lubricants were introduced for use in stern tubes, the probability of a high temperature occurring in the aft stern tube bearing has greatly increased because the performance indexes of these lubricants are not as good as those of traditional mineral lubricants. Given that dynamic behaviour plays an important role in the operation of shaft and bearing systems, their stiffness and damping coefficients should be calculated to determine the design margin of the shaft and bearing system.

The two main types of damage to aft stern tube bearings are fatigue and wiping. Wear of the bearing surface can be prevented by completely separating the bearing and journal through an oil film and accordingly establishing a hydrodynamic lubrication oil film. During the operation of the aft stern tube bearing, the unbalanced force produced by propellers is not constant due to different sea conditions and ship motions. These unbalanced forces act on the hull through the oil film. Therefore, the dynamic characteristics of the lubricant film should be determined to analyse the oil film performance during bearing operation and ensure that the oil film is sufficiently thick.

Local and foreign scholars have conducted numerous studies on the dynamic characteristics of journal bearings [1–5]. Litwin et al. [6] studied the influence of shaft misalignment on water-lubricated sliding bearings. Chatterton et al. [7] performed an experimental investigation on hydrodynamic bearings under severe operation conditions. Jiang [8] and Tang et al. [9] calculated the oil film characteristics of an aft stern tube bearing by adopting the assumed journal centre line position in the calculation and neglecting the journal bending deformation. He et al. [10] conducted the lubrication analysis of aft stern tube bearings with journal deflection. Furthermore, Zhou et al. [11] and Geng et al. [12] considered the oil film reaction force of aft stern tube bearings in shaft alignment calculations, in which the bearings were assumed to be parallel. Zhang et al. [13] and Yang et al. [14] divided the aft stern tube bearing into several bearing segments to calculate the static contact between the bearing and the journal. Yang et al. [15] divided the aft stern tube bearing into several bearing segments and considered the oil film reaction force in the calculation of the shafting alignment, thereby resulting in a reasonable journal centre deflection position. Jakeman [16] presented a nonlinear oil film response model for aft stern tube bearings.

The ultimate purpose of calculating the oil film pressure for journal bearings is to obtain the static and dynamic characteristics through the pressure distribution and its derivatives, as well as to study the stability of the journal bearings. Therefore, journal deflection should be divided into several segments when calculating the dynamic characteristics of the aft stern tube bearings. This deflection is obtained by iteratively solving the Reynolds equation and shaft alignment calculations. Consequently, the dynamic parameters can be obtained.

SOLUTION FOR THE DYNAMIC COEFFICIENT OF JOURNAL BEARINGS

Infinitely wide and long bearing theories can simplify 2D problems into 1D ones to produce analytical solutions. However, only approximate qualitative analyses are available for complicated problems. Therefore, 1D solutions have limitations. Hence, practical results can only be obtained using 2D numerical solutions.

COEFFICIENT FOR DYNAMIC CHARACTERISTICS

Aft stern tube bearings belong to journal bearings. As shown in Fig. 1, under the action of the oil film forces F_y and F_z, the journal centre O_2 rotates at an eccentric position relative to the bearing centre O_1. The figure also illustrates the eccentric distance e, attitude angle θ, inner radius of the bearing R_1, outer radius of the journal R_2, and the radial clearance $c = R_1 - R_2$. The hydrodynamic lubrication film is formed by the relative motion between the inner surface of the bearing and the outer surface of the journal. In addition, the lubrication state belongs to hydrodynamic lubrication. The Reynolds equation can be used to describe the viscous flow phenomena in this narrow gap.

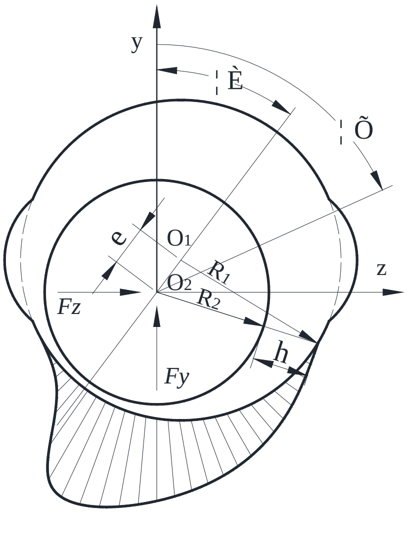

Fig. 1. Shaft centre position

When the journal is disturbed by displacement or velocity at the static equilibrium position, the reaction force that acts on the journal changes. The relationship between the change in force and disturbance is nonlinear. To simplify the analysis, the oil film force can be approximately regarded as a linear function of the small displacement and velocity of the journal when the disturbance is small. The Taylor method is applied to expand the oil film force against the disturbance parameter and maintain the first order as Eq. (1).

$$\begin{cases} F_z = F_{z0} + \left.\dfrac{\partial F_z}{\partial z}\right|_0 \Delta z + \left.\dfrac{\partial F_z}{\partial y}\right|_0 \Delta y + \left.\dfrac{\partial F_z}{\partial \dot{z}}\right|_0 \Delta \dot{z} + \left.\dfrac{\partial F_z}{\partial \dot{y}}\right|_0 \Delta \dot{y} + \cdots \\ F_y = F_{y0} + \left.\dfrac{\partial F_y}{\partial z}\right|_0 \Delta z + \left.\dfrac{\partial F_y}{\partial y}\right|_0 \Delta y + \left.\dfrac{\partial F_y}{\partial \dot{z}}\right|_0 \Delta \dot{z} + \left.\dfrac{\partial F_y}{\partial \dot{y}}\right|_0 \Delta \dot{y} + \cdots \end{cases} \tag{1}$$

where F_z and F_y are the components of the oil film force in the z and y directions, respectively; and F_{z0} and F_{y0} denote the component oil film forces in the z and y directions at the static equilibrium position, respectively.

On the one hand, the coefficient of oil film stiffness is the increment in the oil film force caused by the unit displacement.

$$k_{zz} = \left.\frac{\partial F_z}{\partial z}\right|_0, \; k_{zy} = \left.\frac{\partial F_z}{\partial y}\right|_0, \; k_{yz} = \left.\frac{\partial F_y}{\partial z}\right|_0, \text{ and } k_{yy} = \left.\frac{\partial F_y}{\partial y}\right|_0.$$

On the other hand, the oil film damping coefficient is the increment in oil film force caused by the unit velocity.

$$c_{zz} = \left.\frac{\partial F_z}{\partial \dot{z}}\right|_0, \; c_{zy} = \left.\frac{\partial F_z}{\partial \dot{y}}\right|_0, \; c_{yz} = \left.\frac{\partial F_y}{\partial \dot{z}}\right|_0, \text{ and } c_{yy} = \left.\frac{\partial F_y}{\partial \dot{y}}\right|_0,$$

where the first and second coordinates of each coefficient represent the force and the displacement or velocity direction, respectively.

In addition, k_{zy}, k_{yz} and c_{zy}, c_{yz} are the cross-stiffness and cross-damping/dynamic coefficients, respectively. These coefficients reflect the coupling action of the oil film force in two mutually perpendicular directions (i.e., the incremental direction of the oil film force is inconsistent with the displacement or velocity direction of the journal). The magnitude and sign of the cross-dynamic coefficients affect the bearing's stability.

CALCULATION OF DYNAMIC CHARACTERISTIC COEFFICIENT

If the Reynolds equation of unsteady motion has an analytic solution, such as infinitely long and infinitely short bearings, then the oil film stiffness and damping coefficient can be directly obtained. The equations of the general journal bearings have no analytical solution and can only be solved using numerical methods. For general journal bearings, the commonly used calculation methods include difference, partial derivative, small parameter, and finite element methods. When the difference method is adopted, accuracy depends on the selected disturbance. Partial derivative and small parameter methods must solve the Reynolds equation four times, and the computation speed and precision of both methods are approximately the same. In this study, the small parameter method is used to solve the coefficient of the dynamic characteristics. When the journal is disturbed, the components of the disturbing velocity of the journal centre on the two axes are $\dot{y}$ and $\dot{z}$. If the elastic deformations of the bearing and journal surface are not considered, then the Reynolds equation for the unsteady motion of an incompressible hydrodynamic journal bearing can be expressed as

$$\begin{aligned}&\frac{1}{r^2}\frac{\partial}{\partial \varphi}\left(\frac{h^3}{\eta}\frac{\partial p}{\partial \varphi}\right) + \frac{\partial}{\partial z}\left(\frac{h^3}{\eta}\frac{\partial p}{\partial x}\right) \\ &= 6\omega\frac{\partial h}{\partial \varphi} + 12(\dot{y}\cos\varphi + \dot{z}\sin\varphi)\end{aligned}, \tag{2}$$

where h is the film thickness, p denotes the film pressure, η indicates the dynamic viscosity of the lubricating oil, x represents the axial coordinate, and ω refers to the angular velocity of the journal rotation. Fig. 1 displays the other symbols.

Given $h = cH$, $p = \frac{2\eta\omega}{\psi^2}\bar{p}$, $x = \frac{L}{2}\lambda$, $\dot{z} = c\omega z'$, $\dot{y} = c\omega y'$, $\dot{e} = c\omega y'$, and $\dot{\varphi} = \boldsymbol{\varphi}$ ψ,

where c and L are the half clearance and effective length of the bearing, respectively. φ represents the clockwise rotation angle from the y-axis, and the dimensionless form of Eq. (3) is written as

$$\begin{aligned}&\frac{\partial}{\partial \phi}\left(H^3\frac{\partial \bar{p}}{\partial \varphi}\right) + \left(\frac{D}{L}\right)^2\frac{\partial}{\partial \lambda}\left(H^3\frac{\partial p}{\partial \lambda}\right) \\ &= 3\frac{\partial H}{\partial \varphi} + 6(y'\cos\varphi + z'\sin\varphi)\end{aligned} \tag{3}$$

For the small parameter method, the expressions of oil film thickness and pressure under small displacement and velocity perturbations (only linear terms are retained) are presented as follows.

$H = H_0 + \bar{z}\sin\varphi + \bar{y}\cos\varphi$,

$\bar{p} = \bar{p}_0 + \bar{p}_{\bar{z}}\bar{z} + \bar{p}_{\bar{y}}\bar{y} + \bar{p}_{z'}z' + \bar{p}_{y'}y'$,

where $\bar{p}_{\bar{z}} = \frac{\partial \bar{p}}{\partial \bar{z}}$, $\bar{p}_{\bar{y}} = \frac{\partial \bar{p}}{\partial \bar{y}}$, $\bar{p}_{z'} = \frac{\partial \bar{p}}{\partial z'}$, and $\bar{p}_{y'} = \frac{\partial \bar{p}}{\partial y'}$.

The following equation is obtained by substituting these expressions into Eq. (3) and omitting the higher order as follows.

$$\left[\frac{\partial}{\partial \varphi}\left(H^3\frac{\partial}{\partial \varphi}\right) + \left(\frac{D}{L}\right)^2\frac{\partial}{\partial \lambda}\left(H^3\frac{\partial}{\partial \lambda}\right)\right]\begin{bmatrix}\bar{p}_0 \\ \bar{p}_{\bar{z}} \\ \bar{p}_{\bar{y}} \\ \bar{p}_{z'} \\ \bar{p}_{y'}\end{bmatrix} = \begin{bmatrix}3\frac{\partial H_0}{\partial \varphi} \\ 3\cos\varphi - 9\frac{\sin\varphi}{H_0}\frac{\partial H_0}{\partial \varphi} - 3H_0^3\frac{\partial}{\partial \varphi}\left(\frac{\sin\varphi}{H_0}\right)\frac{\partial \bar{p}_0}{\partial \varphi} \\ -3\sin\varphi - 9\frac{\cos\varphi}{H_0}\frac{\partial H_0}{\partial \varphi} - 3H_0^3\frac{\partial}{\partial \varphi}\left(\frac{\cos\varphi}{H_0}\right)\frac{\partial \bar{p}_0}{\partial \varphi} \\ 6\sin\varphi \\ 6\cos\varphi\end{bmatrix} \tag{4}$$

The first formula refers to the static Reynolds equation, and the four subsequent formulas are the perturbation equations. The stiffness and damping coefficient of the oil film can be obtained by solving the four subsequent formulas and integrating them as Eqs. (5) and (6).

$$\begin{cases} K_{zz} = \int_{-1}^{1}\int_{0}^{2\pi} -\frac{\partial \bar{p}}{\partial \bar{z}}\sin\varphi d\lambda \\ K_{yz} = \int_{-1}^{1}\int_{0}^{2\pi} -\frac{\partial \bar{p}}{\partial \bar{z}}\cos\varphi d\lambda \\ K_{yz} = \int_{-1}^{1}\int_{0}^{2\pi} -\frac{\partial \bar{p}}{\partial \bar{y}}\sin\varphi d\lambda \\ K_{yy} = \int_{-1}^{1}\int_{0}^{2\pi} -\frac{\partial \bar{p}}{\partial \bar{y}}\cos\varphi d\lambda \end{cases} \tag{5}$$

$$\begin{cases} C_{zz} = \int_{-1}^{1}\int_{0}^{2\pi} -\dfrac{\partial \overline{p}}{\partial z'} sin\varphi d\lambda \\ C_{yz} = \int_{-1}^{1}\int_{0}^{2\pi} -\dfrac{\partial \overline{p}}{\partial z'} cos\,\varphi d\lambda \\ C_{yz} = \int_{-1}^{1}\int_{0}^{2\pi} -\dfrac{\partial \overline{p}}{\partial y'} sin\varphi d\lambda \\ C_{yy} = \int_{-1}^{1}\int_{0}^{2\pi} -\dfrac{\partial \overline{p}}{\partial y'} cos\,\varphi d\lambda \end{cases} \quad (6)$$

If the lubrication pressure is expressed by p, then the Reynolds equation is written in standard form as a 2D two-order partial differential equation.

$$A\frac{\partial^2 p}{\partial x^2} + B\frac{\partial^2 p}{\partial y^2} + C\frac{\partial p}{\partial x} + D\frac{\partial p}{\partial y} = E \quad (7)$$

where A, B, C, and D are known variables. The relationship among the variables of each node and the adjacent nodes can be determined by substituting the sum of the difference quotients using the previous equation. This relationship can be written as

$$p_{i,j} = C_N p_{i,j+1} + C_S p_{i,j-1} + C_E p_{i+1,j} + C_W p_{i-1,j} + G \quad (8)$$

$C_N = \left(\dfrac{B}{\Delta y^2} + \dfrac{D}{2\Delta y}\right)\Big/K$, $C_S = \left(\dfrac{B}{\Delta y^2} - \dfrac{D}{2\Delta y}\right)\Big/K$,

$C_E = \left(\dfrac{A}{\Delta z^2} + \dfrac{C}{2\Delta z}\right)\Big/K$, $C_W = \left(\dfrac{A}{\Delta z^2} - \dfrac{C}{2\Delta z}\right)\Big/K$, $G = -\dfrac{E}{K}$, and

$K = 2\times\left(\dfrac{A}{\Delta z^2} + \dfrac{B}{\Delta y^2}\right)$.

The following boundary conditions are used when the oil film force is solved using the static Reynolds equation.

1) Axial direction, $P\big|_{Y=\pm 1/2} = 0$.

2) Circumferential direction, $P\big|_{\varphi=0} = 0$, $P\big|_{\varphi=\varphi 2} = 0$, and $\dfrac{\partial \mathrm{P}}{\partial \theta}\bigg|_{\varphi=\varphi 2} = 0$.

If P < 0 in the iteration for a node, then P = 0. The final location of the oil film is determined after the iteration.

In solving the perturbed Reynolds equation, the perturbation pressure on all boundaries of the entire oil film region is zero, which is basically the boundary condition.

COMPUTATIONAL VALIDATION

In the calculation, the circumferential direction was divided into 72 equal parts, whereas the bearing axial direction was divided into 50 equal parts. The relative accuracy criterion of the Reynolds equation is 1E-6. Table 1 shows the comparison of the calculated results for a circular bearing with L/D = 1, which is adopted from the study by Zhang et al. [17]. The dimensionless coefficients of the dynamic characteristic under different eccentricities (ecc.) are enumerated. The results are nearly the same, except for the results in k_{zy} and k_{yz} and those with 0.95 ecc. Zhang et al. stated that the difference mesh should be finely divided when ecc. is greater than 0.9. For the grid spacing in the circumferential direction, 2–3° spacing is suggested. Therefore, the 5° spacing used in the present work possibly caused the differences. Figs. 2–5 present the distributions of the dimensionless disturbance pressures of the displacement and velocity in the y and z directions when ecc. is 0.4, respectively.

The columns marked with "*" contain the results of this work, whereas those marked with "**" present the results in [17], in which the coefficients are combined given that the cross-damping coefficients are theoretically equal. Moreover, these coefficients are equal to the cross-damping coefficient in the present study, thereby validating the program.

Tab. 1. Comparison of dimensionless dynamic characteristics

ecc	θ		k_{zz}		k_{zy}		k_{yz}		k_{yy}		c_{zz}		c_{zy}	c_{yz}		c_{yy}	
	*	**	*	**	*	**	*	**	*	**	*	**	*	*	**	*	**
0.1	75.3	75.1	0.26	0.27	−0.49	−0.52	1.97	2.07	0.44	0.33	1.00	1.04	0.26	0.26	0.28	3.96	4.15
0.2	64.1	63.6	0.56	0.58	−0.54	−0.60	2.32	2.43	0.98	0.72	1.22	1.27	0.59	0.60	0.62	4.69	4.92
0.3	56.1	55.6	0.96	0.99	−0.63	−0.73	2.92	3.05	1.74	1.26	1.63	1.68	1.10	1.10	1.14	5.96	6.24
0.4	50.3	50.1	1.51	1.50	−0.72	−0.94	3.85	4.01	2.95	2.10	2.25	2.32	1.87	1.87	1.92	7.97	8.32
0.5	45.6	45.3	2.15	2.10	−0.63	−0.82	5.20	5.29	5.16	3.81	2.71	2.51	2.65	2.66	2.43	10.8	11.0
0.6	40.9	40.5	3.16	3.21	−0.40	−0.83	7.58	7.78	9.40	7.15	3.40	3.41	3.93	3.93	3.93	15.8	16.2
0.7	35.9	36.0	4.88	4.98	0.34	−0.20	12.2	12.5	19.0	15.1	4.18	4.33	5.78	5.77	5.94	21.2	26.0
0.8	30.3	30.2	8.89	8.97	2.72	2.10	24.2	24.6	47.5	40.2	6.05	5.90	10.4	10.3	10.0	49.2	49.5
0.9	22.8	23.0	24.3	24.9	16.6	14.2	80.3	82.1	206	181	12.2	13.0	28.9	28.5	30.8	158	164
0.95	17.1	18.1	60.4	62.3	77.5	43.1	255	260	890	719	20.2	32.8	65.8	63.5	99.9	468	514

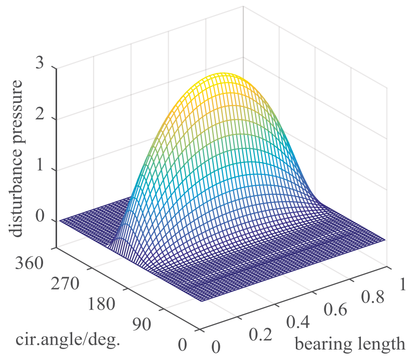

Fig. 2. Displacement disturbance in the z direction

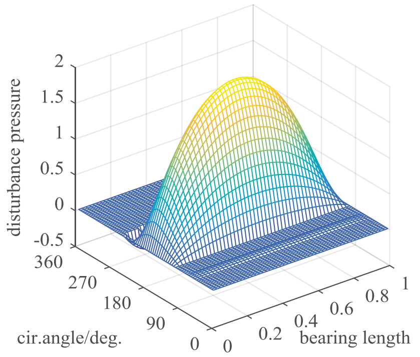

Fig. 3. Displacement disturbance in the y direction

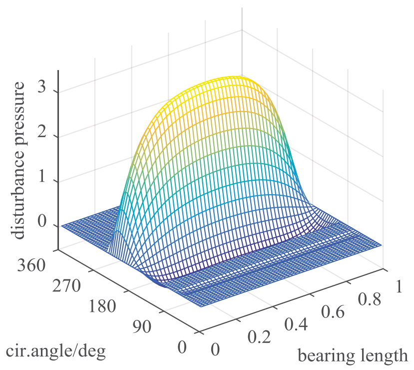

Fig. 4. Velocity disturbance in the z direction

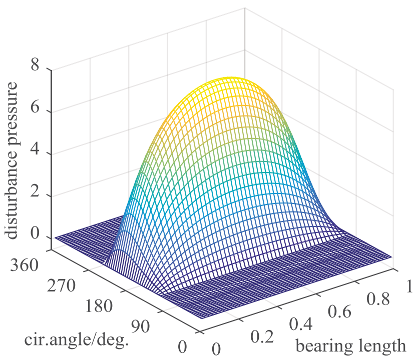

Fig. 5. Velocity disturbance in the y direction

SOLUTION FOR THE JOURNAL DEFLECTION

To solve the journal deflection, the oil film reaction force of the aft stern tube bearing is considered in the calculation of shaft alignment. The aft stern tube bearing is divided into several segments. The deflection in the journal's centre line is characterised by the midpoint of the bearing sections. Then, the oil film thickness is obtained and the oil film force is calculated to solve the static Reynolds equation. The convergence solution for the final midpoint locations can be obtained through the iterative process between the shaft alignment calculation and the Reynolds equation. Fig. 6 presents the flow chart of the process.

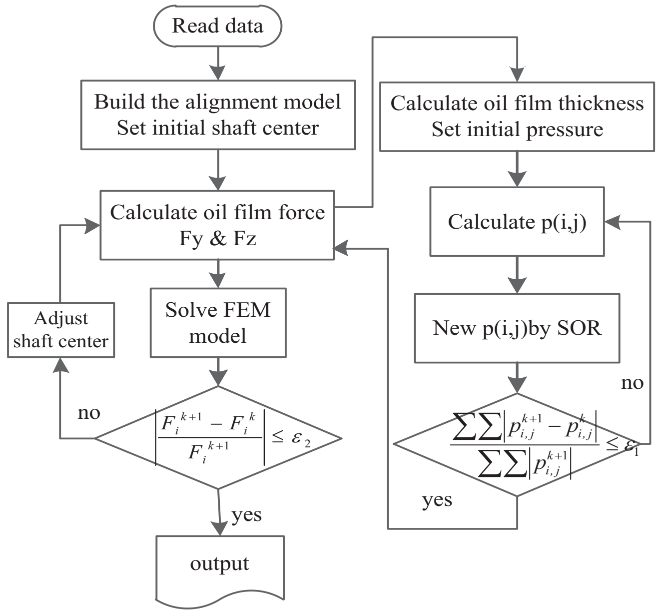

Fig. 6. Flow chart

EXAMPLE

This study takes the propulsion shafting system of a second-generation 400k very large ore carrier as an example (Fig. 7). The major information of shafting, which uses the main engine MAN 7G80ME to directly drive the single propeller with a maximum continued revolution of 58 r/min, is listed in Table 2. The propulsion shafting is composed of a propeller shaft, intermediate shaft, and crankshaft. Moreover, white metal-type journal bearings, such as the aft stern tube, forward stern tube, and intermediate shaft bearings, are arranged. The bearings are numbered from small to large from the aft side to the forward side. In accordance with the MDT's recommendation, six main engine bearings are selected, and nine bearings are included in the calculation of shaft alignment.

Tab. 2. Major information of shafting

Item	Content
Oil viscosity	100 cst @ 40°C
Propeller	Diameter:11.2 m Weight:69.45 ton (in air)
Propeller shaft	Diameter × length: Φ890 mm ×10990 mm
Intermediate shaft	Diameter × length: Φ680 mm ×10880 mm
Aft stern tube bearing	Inner diameter × length: Φ891.2 mm × 1850 mm
Forward stern tube bearing	Inner diameter × length: Φ894.2 mm × 670 mm

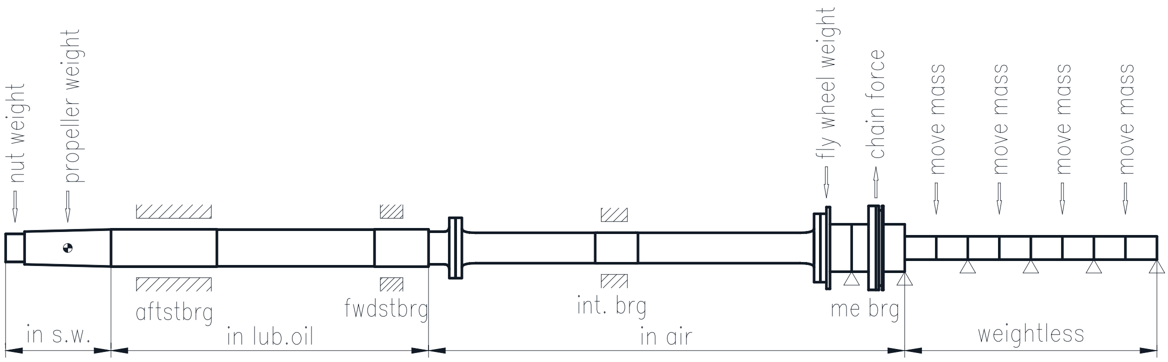

Fig. 7. Shaft alignment calculation model

When the propeller is working at the stern of the ship, unbalanced force and moment are produced because of the non-uniform flow field (Fig. 8). The propeller's Cartesian coordinate system is defined as follows. The x-axis coincides with the centre line of the shaft system, pointing to the bow. The coordinate's origin O is located at the propeller disc, with the y-axis in the straight up direction and the z-axis at the starboard. In the calculation of the shafting alignment, the moments in the y and z directions are considered. When the shaft rotational speed is 58 r/min, My = 405 kN·m and Mz = −721 kN·m. The calculated moment of the other revolutions can be converted on the basis of the quadratic relationship.

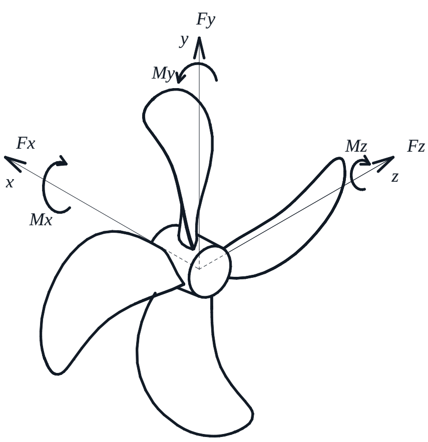

Fig. 8. Unbalanced force and moment on the propeller

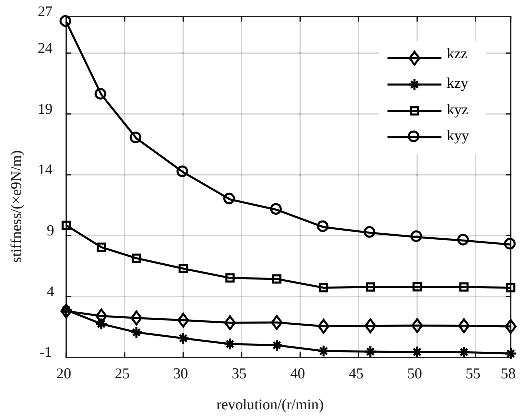

Fig. 9. Stiffness of the aft stern tube bearing

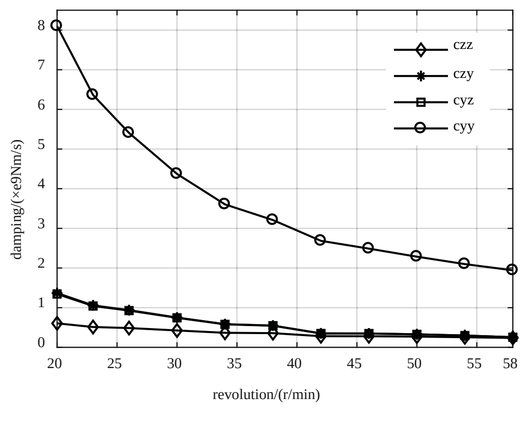

Fig. 10. Damping of the aft stern tube bearing

Figs. 9 and 10 show the relationships of the stiffness and damping of the aft stern tube bearing with revolutions. The lower the number of revolutions is, the thinner the oil film thickness required to produce a similar oil film lift force, which will result in the low relative position of the journal in the aft stern tube bearing, as well as an evident increase in the stiffness and damping in the vertical direction. In addition, the cross-stiffness is not zero, thereby causing journal whirling. The journal stability can be assessed on the basis of the calculated values of stiffness and damping for the oil film of the aft stern tube bearing at each revolution.

In the calculation of the whirling vibration for marine propulsion shafting, the support stiffness of the aft stern tube bearing is often considered the same within the calculated revolution range, and the difference between the vertical and horizontal directions is neglected. However, in this example, the vertical support stiffness of the aft stern tube bearing, which is several times the horizontal support stiffness, changes with the different number of revolutions. The higher the number of revolutions, the smaller the stiffness. Therefore, the present work is helpful in accurately calculating the whirling vibration of the ship propulsion shafting.

Considering that the length and diameter ratio of the aft stern tube bearing is approximately 2, the aft stern tube bearing is divided into 20 sub-bearing segments. The obtained stiffness and damping values of each bearing segment are shown in Figs. 11 and 12, respectively. In Figs. 10 and 12, the cross-damping is equal. This result is consistent with the theoretical qualitative conclusion. Moreover, the accuracy of the calculation program is verified.

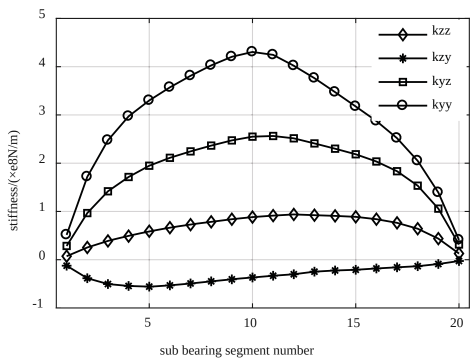

Fig. 11. Bearing segment stiffness

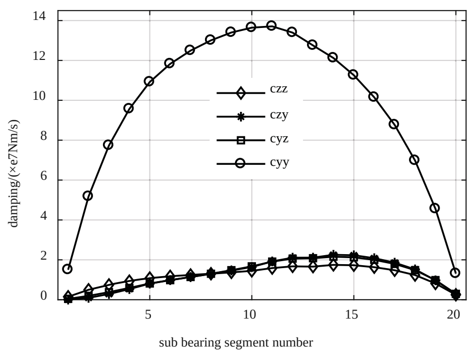

Fig. 12. Bearing segment damping

The journal centre trajectory is compared with the journal that was considered as a straight line.To obtain the result for the journal centre without considering journal deflection, the modulus of elasticity of the journal part was set to 1,000 times the normal value to increase the stiffness of the shaft. The journal centre was presented by the midpoints of the sub-bearing segments. In Fig. 13, case "1" refers to the result for considering journal deflection, whereas case "2" corresponds to the result without considering journal deflection at 20 r/min. The journal centres are different. The journal centre line bends in the y direction in case "1" due to the bending moment caused by the heavy propeller. By contrast, the line is straight in case 2. Furthermore, given that the bending moment in the z direction is small, no evident deflection was observed in this direction.

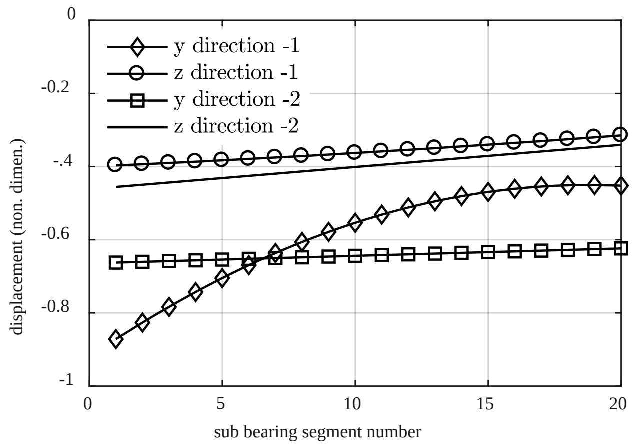

Fig. 13. Comparison of journal centre displacement

Fig. 14 presents the comparison of the minimum oil film thickness and maximum oil film pressure along the bearing axis direction. Because of the journal deflection, the edge load occurs at the after end of the aft stern tube bearing, which is obviously at the very low revolutions of 20 r/min. Therefore, a reasonable result is obtained by considering the bearing journal deflection. Consequently, precise dynamic characteristics are obtained.

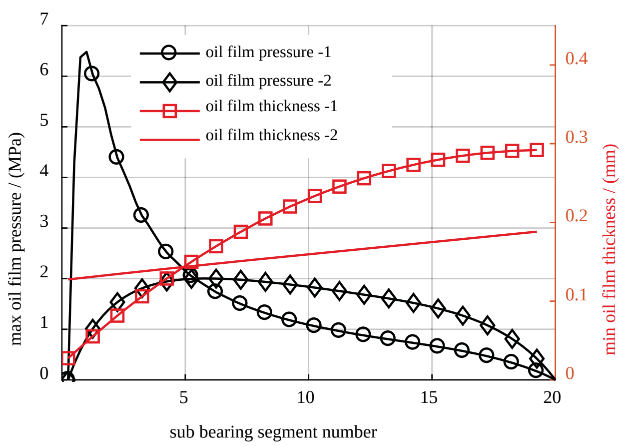

Fig. 14. Comparison of the minimum oil film thickness and maximum oil film pressure

Given the varying pressure distribution when the deflection of the bearing is neglected, the stiffness and damping values will also be different. The results of the dimensionless stiffness at 20 r/min with and without considering journal deflection are displayed in Figs. 15 and 16, respectively. The stiffness curve is similar to the maximum pressure line in Fig. 14. The stiffness is affected by the edge load effect when the deflection of the journal centre line is considered, thereby increasing the stiffness at the after part. Moreover, the pressure disturbance is large when the deflection of the journal centre line is considered because of the high local pressure.

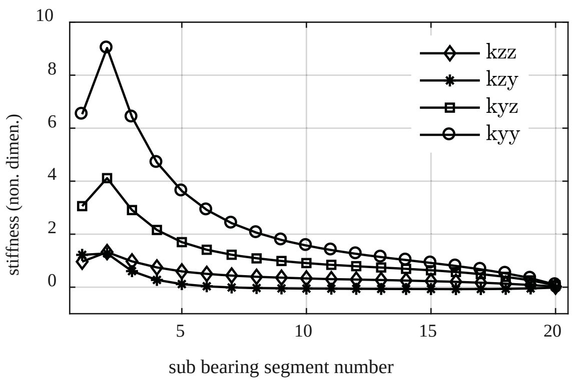

Fig. 15. Bearing segment stiffness when journal deflection is considered

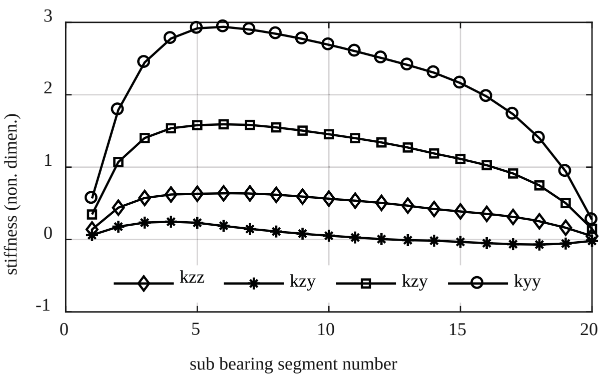

Fig. 16. Bearing segment stiffness when journal deflection is neglected

CONCLUSION

Dynamic performance is crucial to the working reliability of aft stern tube bearings. The deflection of the journal should be considered to obtain accurate and reliable dynamic characteristics.

The reasonable journal deflection of the aft stern tube bearing can be obtained from the iteration between the shafting alignment and the Reynolds equation.

The calculation of the dynamic characteristics of the aft stern tube bearings provides the foundation for the calculation of the journal trajectory, as well as a reliable stiffness value for the calculation of the whirling vibration. In the past, the stiffness of the aft stern tube bearing was an assumed value, but in the future, each case can be separately considered and accurate calculation results can be obtained.

ACKNOWLEDGEMENTS

This work is funded by the Ministry of Industry and Information "Marine low speed diesel engine (first phase)."

REFERENCES

1. Wang D., Zhu J. A. (1995): *Finite element method for computing dynamic coefficient of hydrodynamic journal bearing.* Journal of Aerospace Power, 3, 272-274 (in Chinese).

2. Shi D. Y., Zhang C., Ren L. L., et al. (2011): *Research on the oil film pressure and dynamic coefficient of a sliding bearing.* Journal of Harbin Engineering University, 9, 1134-1139 (in Chinese).

3. Wang J. K., Khonsari M. K. (2006): *A new derivation for journal bearing stiffness and damping coefficients in polar coordinates.* Journal of Sound and Vibration, 290, 500-507.

4. Zhang X. L., Yin Z. W., Gao G. Y., et al. (2015): *Determination of stiffness coefficients of hydrodynamic water-lubricated plain journal bearings.* Tribology International, 85, 37-47.

5. Litwin W., Olszewski A., Wodtke M. (2012): *Influence of Shaft Misalignment on Water Lubricated Turbine Sliding Bearings with Various Bush Modules of Elasticity.* Key Engineering Materials, 490, 128-140.

6. Meruane V., Pascual R. (2008): *Identification of nonlinear dynamic coefficients in the plain journal bearings.* Tribology International, 41, 743-754.

7. Chatterton S. Dang P. V., Pennacchi P., et al. (2017): *Experimental evidence of a two-axial groove hydrodynamic journal bearing under severe operation conditions.* Tribology International, 109, 416-427.

8. Jiang R. Y. (1984): *Calculation of hydro-static and dynamic characteristics of marine stern tube bearing by finite method.* Journal of Wuhan Institute of Water Transportation Engineering, 1, 45-56 (in Chinese).

9. Tang Y. M., Hai P. Z., Jin Z. H. (1983): *Analysis and calculation of lubrication characteristics of marine stern tube bearing.* Journal of Wuhan Institute of Water Transportation Engineering, 4, 9-20 (in Chinese).

10. He T., Zou D. Q., Lu X.Q., et al. (2013): *Mixed lubrication analysis of ship stern tube bearing considering bending of shaft.* Journal of Harbin Engineering University, 1, 104-109 (in Chinese).

11. Zhou R. P., Li B. R., Li Z. G. (2005): *The analysis of influence of oil film on the propulsion shafting alignment of vessels*. Ship & Ocean Engineering, 2005(4), 64-67 (in Chinese).

12. Geng H. C., Rao Z. S., Cui S. (2004): *Oil film calculation and reaction analyses for marine shaft system*. Journal of Ship Mechanics, 5, 120-124 (in Chinese).

13. Zhang M., Zhang G. H., Liu Z. S. (2016): *Research on large ship propulsion shafting alignment multi-nonlinear-elastic support model*. Journal of Ship Mechanics, 1-2, 176-183 (in Chinese).

14. Yang H. J., Lu F., Che C. D. (2018): *Alignment calculation for ship propulsion shaft based on segmentation elastic contact theory of aft stern tube bearing*. Journal of Shanghai Jiao Tong University, 6, 681-686.

15. Yang H. J., Wang W. Z., Li J., et al. (2018): *Calculation of shaft alignment with considering of oil film force of stern tube bearing*. Ship Building of China, 1,142-150.

16. Jakeman R. W. (1989): *Non-linear oil film response model for dynamically misaligned stern tube bearing*. Tribology International, 1, 1-8.

17. Zhang Z. M., Zhang Y. Y., Xie Y. B., et al. (1986): *Hydrodynamic lubrication theory of journal bearing*, Higher Education Press, Beijing.

CONTACT WITH THE AUTHORS

Hongjun Yang
e-mail: yhj99373aman@163.com
Shanghai Merchant Ship Design & Research Institute,
2633 Zuchongzhi Road, 201203 Shanghai,
China

Jun Li
e-mail: sd2@sdari.com.cn
Shanghai Merchant Ship Design & Research Institute,
2633 Zuchongzhi Road, 201203 Shanghai,
China

Xiaolong Li
e-mail: lixiaolong@nacks.com
Nantong COSCO KHI Ship Engineering Co.,Ltd.
Jiangsu Nantong, China.,
901 Changjiang Middle Road,
226005 Nantong, Jiangsu Province,
China